ChemComm

COMMUNICATION

View Article Online
View Journal | View Issue

Open Access Article. Published on 20 June 2018. Downloaded on 5/14/2026 6:24:47 PM.
This article is licensed under a Creative Commons Attribution-NonCommercial 3.0 Unported Licence.

Check for updates

Cite this: *Chem. Commun.*, 2018, **54**, 7826

Received 12th June 2018,
Accepted 19th June 2018

DOI: 10.1039/c8cc04703k

rsc.li/chemcomm

Isotope effects on the spin dynamics of single-molecule magnets probed using muon spin spectroscopy†

Lorenzo Tesi,[a] Zaher Salman,*[b] Irene Cimatti,[a] Fabrice Pointillart,[c] Kevin Bernot,[c] Matteo Mannini[a] and Roberta Sessoli*[a]

Muon spin relaxation (μSR) experiments on a single-molecule magnet enriched in different Dy isotopes detect unambiguously the slowing down of the zero field spin dynamics for the non-magnetic isotope. This occurs in the low temperature regime dominated by quantum tunnelling, in agreement with previous ac susceptibility investigations. In contrast to the latter, however, μSR is sensitive to all fluctuation modes affecting the lifetime of the spin levels.

Single-Molecule Magnets (SMMs) are transition metal or lanthanide-based systems characterized by a large magnetic moment whose dynamics is governed by magnetic anisotropy which creates a double well energy potential.[1] Through a rational chemical design, anisotropy barriers exceeding a thousand Kelvin have been obtained and blocking of the magnetization observed at a temperature as high as 60 K.[2] The quantum nature of SMMs, however, dominates the low temperature regime revealing themselves in many fascinating effects related to under-barrier mechanisms of relaxation.[3] Among them, quantum tunnelling of electronic magnetization was found to be very sensitive to the environment and in particular to the presence of nuclear spins. The acceleration of the quantum tunnelling in an isotopically enriched Fe_8 SMM using ^{57}Fe (nuclear spin value $I = 1/2$) was for the first time evidenced by measuring the time dependence of magnetization.[4] Following this, the quantum tunnelling between hyperfine levels was also investigated in detail in lanthanide-based SMMs.[5] More recently the spin dynamics of some SMMs comprising either ^{161}Dy ($I = 5/2$) or ^{164}Dy ($I = 0$) tri-positive ions has been investigated by using alternate current (ac) susceptometry. Also in this case quantum tunnelling relaxation was slowed down by reducing the hyperfine field.[6,7] Furthermore, the control of the nuclear magnetic environment is crucial to enhance the quantum coherence in spin systems which can be potentially employed as quantum bits in quantum information technology.[8]

The great appeal of molecular spins to store information or to be operated in quantum gates requires addressing individual or arrays of molecules, for instance by creating monolayer deposits on a surface[9] or embedding a molecule inside an electrical junction.[10] In these cases different tools need to be developed to investigate the spin dynamics. Going beyond the use of XMCD and other synchrotron-based characterization tools, often used to study SMM dynamics on a nanoscale,[11] Muon Spin Relaxation (μSR) emerges as a powerful and versatile technique. In μSR, fully spin-polarized muons, which are positively charged elementary particles with spin value $\frac{1}{2}$, are implanted in the sample. The spin of the implanted muons interacts with the magnetic fields produced by nearby molecules which govern its temporal evolution.[12] The implanted muons decay into positrons (mean lifetime $\sim$2.2 μs), which are emitted preferentially along the muon spin direction at the time of decay. Thus, using appropriately positioned detectors it is possible to reconstruct the time dependence profile of muon spin polarization.

This technique has been extensively employed to characterize the magnetic behaviour of SMMs,[13,14] since it allows a direct investigation of the magnetization dynamics of individual molecules and on a time scale faster than what is currently accessible by magnetic techniques like ac susceptometry. Furthermore, thanks to the possibility of controlling the muon implantation energy, μSR has also been used to investigate depth resolved magnetic properties of thin films of $TbPc_2$ evidencing the critical role of the packing of the molecules.[15] Another Ln-based complex investigated using this technique is $[Dy(hfac)_3(PyNO)]_2$ (DyPyNO), where PyNO = pyridine-*N*-oxide and $hfac^-$ = hexafluoroacetylacetonate. Interestingly, this SMM exhibited the same magnetic behaviour, in the entire temperature range, in bulk and sublimated thin film forms. Moreover, depth resolved experiments provided a homogeneous response from the whole SMM film volume.[16]

[a] *Department of Chemistry "U. Schiff" – Università degli Studi di Firenze and INSTM UdR Firenze, Via della Lastruccia 3, 50019, Sesto Fiorentino, Italy. E-mail: roberta.sessoli@unifi.it*
[b] *Laboratory for Muon Spin Spectroscopy, Paul Scherrer Institute, CH-5232 Villigen PSI, Switzerland. E-mail: zaher.salman@psi.ch*
[c] *Université de Rennes, INSA Rennes, CNRS, ISCR (Institut des Sciences Chimiques de Rennes) – UMR 6226, 35000 Rennes, France*

† Electronic supplementary information (ESI) available. See DOI: 10.1039/c8cc04703k

This journal is © The Royal Society of Chemistry 2018

Open Access Article. Published on 20 June 2018. Downloaded on 5/14/2026 6:24:47 PM.
This article is licensed under a Creative Commons Attribution-NonCommercial 3.0 Unported Licence.

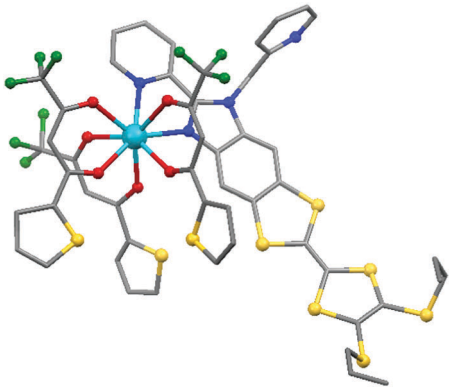

Fig. 1 Molecular structure of Dytta. Turquoise Dy, red O, blue N, green F, yellow S and grey C (for clarity H atoms are omitted).

Although several other SMMs were studied using μSR so far, the effect of nuclear moments on the molecular spin dynamics has not yet been investigated using this technique. In this communication, we show that μSR is able to detect effects of isotopic enrichment on the molecular spin dynamics. Here we report on the μSR investigation of the $[Dy(tta)_3(L)]\cdot C_6H_{14}$ (Dytta) system, where tta^- = 2-thenoyltrifluoroacetonate and L = 4,5-bis(propylthio)-tetrathiafulvalene-2-(2-pyridyl)-benzimidazole methyl-2-pyridine (see Fig. 1).[17] In particular we performed these characterizations on two isotopically enriched variants of this mononuclear complex with ^{161}Dy (I = 5/2) and ^{164}Dy (I = 0), and hereafter referred to as ^{161}Dytta and ^{164}Dytta,[6] respectively. In this system the Dy^{III} ion is connected to three tta^- ions and one bidentate L ligand, as shown in Fig. 1, which could promote the grafting on the gold surface. In this configuration, the metal is at the centre of a N_2O_6 square antiprism environment leading to a D_{4d} local symmetry around the Dy^{III} ion. The J = 15/2 manifold resulting from the spin–orbit coupling of the L = 5 and S = 5/2 of the $4f^9$ configuration is split by the crystalline field. The anisotropic distribution of the electrostatic potential around the Dy^{III} ion stabilizes the Kramers doublet $M_J = \pm 15/2$. This corresponds to an easy axis magnetic anisotropy and effective g values of the ground state $g_x = g_y = 0$ and $g_z \sim 20$. *Ab initio* calculations confirmed this picture and estimated the first excited doublet, $M_J = \pm 13/2$, at ~180 K.[17] Magnetic measurements performed on solid state compounds revealed SMM behaviour, *i.e.* slow relaxation up to 15 K with and without the application of a static magnetic field. Two relaxation mechanisms were evidenced: (i) a thermally activated process, though with an estimated energy barrier much smaller than that estimated from the separation between the ground and first excited doublets, as often observed in highly anisotropic systems,[18] and (ii) a temperature-independent process, attributed to fast quantum tunnelling in zero field.[17] In the latter regime, an increase in the relaxation time of about an order of magnitude was observed when passing from ^{161}Dytta to ^{164}Dytta.[6] In contrast, no isotope effect was evidenced in the thermally activated regime.

Microcrystalline powders of ^{161}Dytta and ^{164}Dytta (see Table S1 for isotope compositions and Fig. S1, ESI† for PXRD spectra) were investigated at the GPS spectrometer of the Paul Scherrer Institute. Conventional bulk μSR measurements (with an implantation energy of ~4 MeV corresponding to a few 100 μm stopping depth) were performed in zero magnetic field (ZF). The time dependence of muon spin polarization, $P_Z(t)$, was recorded as a function of temperature and selected spectra recorded for both samples are presented in Fig. S2 and S3 (ESI†), whereas spectra for all measured temperatures are shown in Fig. S4 and S5 (ESI†). At high temperature $P_Z(t)$ decays exponentially from its initial value to zero, as expected, when the local magnetic field experienced by each muon is fluctuating. As the temperature is decreased, the damping rate of the polarization increases gradually. However, below ~30 K, we find that $P_Z(t)$ exhibits a shallow dip at short times, and then a recovery to ~1/3 followed by slow relaxation at even longer times. As in the case of other SMMs, $P_Z(t)$ can be fitted throughout the full temperature range using a phenomenological Kubo–Toyabe model[19] multiplied by a square root exponential relaxation function[15,16]

$$P_Z(t) = \left[\frac{1}{3} + \frac{2}{3}(1 - \Delta t)e^{-\Delta t}\right] e^{-\sqrt{\lambda t}}. \quad (1)$$

This function accounts for depolarization due to a Lorentzian distribution of local static magnetic fields of width Δ, with an additional relaxation, λ, due to fluctuating magnetic field components from the Dy^{III} magnetic moments. The square root in the dynamic component originates from averaging many inequivalent sites of the molecule where muons can stop.[20,21] Best fits of $P_Z(t)$ (see the ESI† for details) provide the values of Δ and λ as a function of temperature, as shown in Fig. 2, and exhibit similar behaviour to other investigated SMMs.[14–16,21] These parameters are representative of the magnetic properties and spin dynamics of the single-molecule, since each implanted muon is sensitive to the dipolar fields

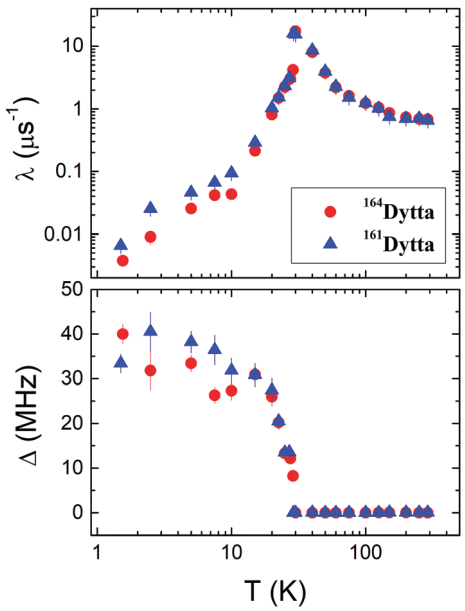

Fig. 2 Temperature dependence of the relaxation rate (top) and width of local static magnetic field distribution (bottom) for ^{164}Dytta and ^{161}Dytta measured using μSR in zero field.

Open Access Article. Published on 20 June 2018. Downloaded on 5/14/2026 6:24:47 PM.
This article is licensed under a Creative Commons Attribution-NonCommercial 3.0 Unported Licence.

from its nearest neighbour. The temperature dependences of Δ and λ reflect the gradual evolution of Dy^{III} spin dynamics, from fast fluctuating spins at high temperature to a quasi-static (*i.e.* very slow dynamics) at low temperature. We outline three specific regimes: (i) at high temperatures fast thermally activated spin fluctuations dominate, with $\Delta = 0$, *i.e.* no local static magnetic fields probed by muons, and a relatively small λ. The latter increases upon decreasing the temperature due to the slowing down of the fluctuations of the Dy^{III} magnetic moments on a time scale comparable with the muon spin Larmor precession frequency. (ii) Around 30 K, λ exhibits a narrow peak coinciding with an abrupt increase (non-zero value) in Δ, which corresponds to the appearance of static magnetic fields. (iii) Finally, at low temperature, large quasi-static fields (large Δ) are experienced by muons together with a pronounced decrease of λ.

Although no significant dissimilarities are observed in the high temperature region, below ~15 K a clear difference emerges, exceeding the experimental uncertainty and revealing a larger dynamic relaxation parameter λ for ^{161}Dytta. In a similar way to what is observed in ac susceptibility measurements, the isotope effect is visible in the temperature region where under-barrier relaxation dominates. However, when comparing ^{161}Dytta to ^{164}Dytta, only an increase by a factor of ~2 is observed in λ, to be compared with a factor of ~10 for the relaxation time of the bulk magnetization detected by ac susceptometry.[6]

The isotope effect is also evident below 15 K when looking at the correlation time, τ, of the local magnetic field experienced by muons, as shown in Fig. 3 (full temperature range data are reported in Fig. S7, ESI†). This parameter can be extracted from the μSR spectra assuming two different regimes. At low temperature, where quasi-static magnetic fields dominate, the correlation time depends only on λ as $\tau = 2/(3\lambda)$, whereas at high temperature, where thermal fluctuations dominate, $\tau = \lambda/2\Delta_0^2$. Here Δ_0 is the size of the fluctuating field, whose value can be estimated from the saturation value of Δ extrapolated at low temperature. This was taken to be ~35 MHz for both ^{164}Dytta and ^{161}Dytta. Note that there is some scatter in Δ at low temperature since it is on the limit of what is measurable using μSR. However, the exact value of Δ_0 will only affect our estimates of τ at high temperature by up to 10–20%. Moreover, the fact that λ and Δ are the same at high temperature supports our conclusion regarding the lack of the isotope effect at high temperature.

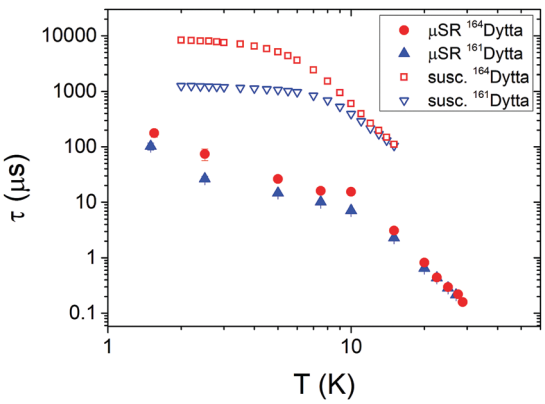

Fig. 3 Correlation time extracted from μSR and relaxation time of magnetization obtained from ac susceptibility as a function of temperature for ^{161}Dytta and ^{164}Dytta. Data are reported on a log–log scale.

It is interesting to note that the extracted τ captures the dynamics of the Dy^{III} magnetic moments but not necessarily in the same way as bulk magnetic measurements do. Indeed, the extracted correlation times are about 1–2 order of magnitude shorter than those extracted from ac susceptibility (Fig. 3). We point out that whereas ac susceptibility is sensitive to excitations with wave-vector $q = 0$, μSR (as a local probe) is sensitive to excitations integrated over all q values of the Brillouin zone.[22] This difference is however not relevant for pure paramagnetic solids, *i.e.* where intermolecular interactions are negligible. In the case of Dytta it has been observed that dipolar interactions, though weak, play a relevant role in the dynamics at low temperature, where quantum tunnelling is dominating. In contrast, the τ extracted from μSR data is shorter over the entire investigated temperature range. To reconcile ac susceptometry and μSR results we should consider that the former is mainly sensitive to relaxation processes that reverse the magnetization, *i.e.* inter-well transitions changing the sign of the spin projection along the anisotropy axis. In fact, in zero field, the equilibrium population of excited spin levels is practically unaffected by the weak oscillating field. In contrast μSR, beyond probing faster dynamics, is sensitive to all types of fluctuations which affect the lifetime of the spin states, including intra-well transitions as well as decoherence. It is therefore not surprising to observe a less pronounced isotope effect by μSR. The hyperfine fields are in fact crucial to establish the resonant condition for the reversal of magnetization by quantum tunnelling, but they are expected to have less influence on the lifetime (or width) of the states. Indeed, it is well known that nuclei, which are not strongly coupled with the electronic spins, provide the largest contribution to decoherence.[23] Finally, it should be remarked that other nuclei, such as ^{1}H and ^{19}F, may affect the electronic spin dynamics of the Dy^{III} ion, but this would not explain the difference between the two samples or the different τ values measured using μSR and ac susceptometry.

As evident from Fig. 3, τ values from μSR show more pronounced temperature dependence than ac susceptibility data below 10 K. This is also in agreement with the sensitivity of muons for intra-well transitions. Similar low temperature behaviour has been observed also for the DyPyNO SMM.[16] The latter has an energy separation between the ground doublet with $M_J = \pm 15/2$ and the first excited doublet with $M_J = \pm 13/2$ of ~170 K, comparable to that calculated for Dytta SMMs. Interestingly, μSR data of $TbPc_2$, which has a much larger separation (~800 K) between the ground and first excited doublets, show that τ is fully saturated below 50 K.[15] Moreover, the τ value of $TbPc_2$ obtained using μSR is closer to that obtained using ac susceptometry applying a magnetic field of 1 kG.[14]

To summarize, our μSR investigation confirms the capability of the technique to capture fine details of the spin dynamics of molecular systems, down to the isotopic effects in the tunnelling

 This journal is © The Royal Society of Chemistry 2018

Open Access Article. Published on 20 June 2018. Downloaded on 5/14/2026 6:24:47 PM.
This article is licensed under a Creative Commons Attribution-NonCommercial 3.0 Unported Licence.

of magnetization. Moreover, this alternative way to study the spin dynamics provides a different and complementary perspective compared to traditional magnetometry. This arises from its local probe character and the consequent sensitivity not only to processes which lead to magnetization reversal but to all sources of spin fluctuations. This aspect is of particular interest in light of current trends in using molecular spin systems for quantum information to realize quantum gates.[24] In this respect, the final goal is using single-molecules or isolated supramolecular structures to perform quantum operations. This poses the additional challenge of preserving, in isolated molecules on substrates, not only the memory effect but also an acceptable quantum coherence time. Thanks to the possibility of implanting muons at different energies, they can be used to probe the dynamics of molecules close to a surface or an interface. The μSR technique provides therefore an almost unique tool to obtain information on the lifetime of spin states and how this is affected by the proximity to the substrate.

Part of this work was performed at the Swiss Muon Source (SμS), the Paul Scherrer Institute (PSI, Switzerland), and it was financially supported by the Italian MIUR (PRIN Project 2015 HYFSRT), the ERC Consolidator Grant MULTIPROSMM (Proj. no. 725184) and Institut Universitaire de France (IUF). We would like to thank Prof. Robert Kiefl and Prof. Elvezio Morenzoni for reading and commenting on the manuscript.

Conflicts of interest

There are no conflicts to declare.

Notes and references

1 R. Sessoli, D. Gatteschi, A. Caneschi and M. A. Novak, *Nature*, 1993, **365**, 141.
2 (*a*) C. A. P. Goodwin, F. Ortu, D. Reta, N. F. Chilton and D. P. Mills, *Nature*, 2017, **548**, 439; (*b*) F. S. Guo, B. M. Day, Y. C. Chen, M. L. Tong, A. Mansikkamäki and R. A. Layfield, *Angew. Chem., Int. Ed.*, 2017, **56**, 11445.
3 (*a*) L. Thomas, F. Lionti, R. Ballou, D. Gatteschi, R. Sessoli and B. Barbara, *Nature*, 1996, **383**, 145; (*b*) J. R. Friedman, M. P. Sarachik, J. Tejada and R. Ziolo, *Phys. Rev. Lett.*, 1996, **76**, 3830; (*c*) W. Wernsdorfer and R. Sessoli, *Science*, 1999, **284**, 133.
4 W. Wernsdorfer, A. Caneschi, R. Sessoli, D. Gatteschi, A. Cornia, V. Villar and C. Paulsen, *Phys. Rev. Lett.*, 2000, **84**, 2965.
5 (*a*) N. Ishikawa, M. Sugita and W. Wernsdorfer, *J. Am. Chem. Soc.*, 2005, **127**, 3650; (*b*) F. Luis, M. J. Martínez-Pérez, O. Montero, E. Coronado, S. Cardona-Serra, C. Martí-Gastaldo, J. M. Clemente-Juan, J. Sesé, D. Drung and T. Schurig, *Phys. Rev. B: Condens. Matter Mater. Phys.*, 2010, **82**, 060403.
6 F. Pointillart, K. Bernot, S. Golhen, B. Le Guennic, T. Guizouarn, L. Ouahab and O. Cador, *Angew. Chem., Int. Ed.*, 2015, **54**, 1504.
7 (*a*) G. Huang, X. Yi, J. Jung, O. Guillou, O. Cador, F. Pointillart, B. Le Guennic and K. Bernot, *Eur. J. Inorg. Chem.*, 2018, 326; (*b*) Y. Kishi, F. Pointillart, B. Lefeuvre, F. Riobe, B. Le Guennic, S. Golhen, O. Cador, O. Maury, H. Fujiwara and L. Ouahab, *Chem. Commun.*, 2017, **53**, 3575.
8 J. M. Zadrozny, J. Niklas, O. G. Poluektov and D. E. Freedman, *ACS Cent. Sci.*, 2015, **1**, 488.
9 (*a*) A. Cornia and M. Mannini, in *Molecular Nanomagnets and Related Phenomena*, ed. S. Gao, Structure and Bonding, Springer, Berlin, Heidelberg, 2014, vol. 164, pp. 293–330; (*b*) R. J. Holmberg and M. Murugesu, *J. Mater. Chem. C*, 2015, **3**, 11986.
10 (*a*) E. Burzurí, A. S. Zyazin, A. Cornia and H. S. J. van der Zant, *Phys. Rev. Lett.*, 2012, **109**, 147203; (*b*) R. Vincent, S. Klyatskaya, M. Ruben, W. Wernsdorfer and F. Balestro, *Nature*, 2012, **488**, 357.
11 (*a*) A. Cini, M. Mannini, F. Totti, M. Fittipaldi, G. Spina, A. Chumakov, R. Rüffer, A. Cornia and R. Sessoli, *Nat. Commun.*, 2018, **9**, 480; (*b*) M. Mannini, F. Pineider, C. Danieli, F. Totti, L. Sorace, P. Sainctavit, M. A. Arrio, E. Otero, L. Joly, J. C. Cezar, A. Cornia and R. Sessoli, *Nature*, 2010, **468**, 417.
12 S. J. Blundell, in *Magnetism: Molecules to Materials*, ed. J. S. Miller and M. Drillon, Wiley-VCH, Weinheim, 2001, pp. 235–256.
13 (*a*) S. J. Blundell, F. L. Pratt, I. M. Marshall, C. A. Steer, W. Hayes, J. F. Letard, S. L. Heath, A. Caneschi and D. Gatteschi, *Synth. Met.*, 2003, **133**, 531; (*b*) F. Branzoli, M. Filibian, P. Carretta, S. Klyatskaya and M. Ruben, *Phys. Rev. B: Condens. Matter Mater. Phys.*, 2009, **79**, 220404; (*c*) Z. Salman, S. R. Giblin, Y. Lan, A. K. Powell, R. Scheuermann, R. Tingle and R. Sessoli, *Phys. Rev. B: Condens. Matter Mater. Phys.*, 2010, **82**, 174427; (*d*) T. Lancaster, S. J. Blundell, F. L. Pratt, I. Franke, A. J. Steele, P. J. Baker, Z. Salman, C. Baines, I. Watanabe, S. Carretta, G. A. Timco and R. E. P. Winpenny, *Phys. Rev. B: Condens. Matter Mater. Phys.*, 2010, **81**, 140409.
14 F. Branzoli, P. Carretta, M. Filibian, M. J. Graf, S. Klyatskaya, M. Ruben, F. Coneri and P. Dhakal, *Phys. Rev. B: Condens. Matter Mater. Phys.*, 2010, **82**, 134401.
15 A. Hofmann, Z. Salman, M. Mannini, A. Amato, L. Malavolti, E. Morenzoni, T. Prokscha, R. Sessoli and A. Suter, *ACS Nano*, 2012, **6**, 8390.
16 E. Kiefl, M. Mannini, K. Bernot, X. Yi, A. Amato, T. Leviant, A. Magnani, T. Prokscha, A. Suter, R. Sessoli and Z. Salman, *ACS Nano*, 2016, **10**, 5663.
17 T. T. da Cunha, J. Jung, M.-E. Boulon, G. Campo, F. Pointillart, C. L. M. Pereira, B. Le Guennic, O. Cador, K. Bernot, F. Pineider, S. Golhen and L. Ouahab, *J. Am. Chem. Soc.*, 2013, **135**, 16332.
18 A. Lunghi, F. Totti, R. Sessoli and S. Sanvito, *Nat. Commun.*, 2017, **8**, 14620.
19 R. Kubo, *Hyperfine Interact.*, 1981, **8**, 731.
20 (*a*) A. Keren, *Phys. Rev. B: Condens. Matter Mater. Phys.*, 1994, **50**, 10039; (*b*) Y. J. Uemura, T. Yamazaki, D. R. Harshman, M. Senba and E. J. Ansaldo, *Phys. Rev. B: Condens. Matter Mater. Phys.*, 1985, **31**, 546.
21 Z. Salman, A. Keren, P. Mendels, V. Marvaud, A. Scuiller, M. Verdaguer, J. S. Lord and C. Baines, *Phys. Rev. B: Condens. Matter Mater. Phys.*, 2002, **65**, 132403.
22 (*a*) T. Moriya, *J. Phys. Soc. Jpn.*, 1963, **18**, 516; (*b*) Y. J. Uemura, *Hyperfine Interact.*, 1984, **18**, 447.
23 M. J. Graham, C.-J. Yu, M. D. Krzyaniak, M. R. Wasielewski and D. E. Freedman, *J. Am. Chem. Soc.*, 2017, **139**, 3196.
24 (*a*) J. Ferrando-Soria, E. M. Pineda, A. Chiesa, A. Fernandez, S. A. Magee, S. Carretta, P. Santini, I. J. Vitorica-Yrezabal, F. Tuna, G. A. Timco, E. J. L. McInnes and R. E. P. Winpenny, *Nat. Commun.*, 2016, **7**, 11377; (*b*) C. Godfrin, A. Ferhat, R. Ballou, S. Klyatskaya, M. Ruben, W. Wernsdorfer and F. Balestro, *Phys. Rev. Lett.*, 2017, **119**, 187702; (*c*) M. Atzori, A. Chiesa, E. Morra, M. Chiesa, L. Sorace, S. Carretta and R. Sessoli, *Chem. Sci.*, 2018, DOI: 10.1039/C8SC01695J.